Journal of Hydrology 564 (2018) 99–114

Contents lists available at ScienceDirect

Journal of Hydrology

journal homepage: www.elsevier.com/locate/jhydrol

Research papers

Geochemical characterization and modeling of regional groundwater contributing to the Verde River, Arizona between Mormon Pocket and the USGS Clarkdale gage

Kimberly R. Beisner[a,*], W. Payton Gardner[b], Andrew G. Hunt[c]

[a] US Geological Survey, 6700 Edith Blvd NE, Albuquerque, NM 87113, USA
[b] University of Montana, Charles H. Clapp Building 353, Missoula, MT 59812, USA
[c] US Geological Survey, Denver Federal Center, Building 95, MS 963, Denver, CO 80225, USA

ARTICLE INFO

This manuscript was handled with the assistance of Fereidoun Rezanezhad, Associate Editor

Keywords:
Radon
Helium
Groundwater discharge
Geochemistry
Groundwater

ABSTRACT

We use synoptic surveys of stream discharge, stable isotopes, and dissolved noble gases to identify the source of groundwater discharge to the Verde River in central Arizona. The Verde River more than doubles in discharge in Mormon Pocket over a 1.4 km distance that includes three discrete locations of visible spring input to the river and other diffuse groundwater inputs. A detailed study of the Verde River between Mormon Pocket and the USGS Clarkdale Gage was conducted to better constrain the location of groundwater inputs, the geochemical signature and constrain the source of groundwater input. Discharge, water quality parameters (temperature, pH, specific conductance, and dissolved oxygen), stable isotopes ($\delta^{18}O$ and $\delta^{2}H$), noble gases (He, Ne, Ar, Kr and Xe), and radon (^{222}Rn) from river water were collected. Groundwater samples from springs and wells in the area were collected and analyzed for tracers measured in the stream along with some additional analytes (major ions, strontium isotopes ($^{87}Sr/^{86}Sr$), carbon-14, $\delta^{13}C$, and tritium). Groundwater isotopic signature is consistent with a regional groundwater source. Groundwater springs discharging to the river have a depleted stable isotopic signature indicating recharge source up to 1000 m higher than the discharge location in the Verde River and are significantly fresher than stream water. Spring water has a radiocarbon age of several thousand years and some areas have tritium less than the laboratory reporting level or low concentrations of tritium (1.5 TU). The strontium isotopes indicate groundwater interaction with tertiary volcanic rock and Paleozoic sedimentary rocks. Along the study reach with distance downstream, Verde stream water chemistry shows increased ^{222}Rn, freshening, increased ^{4}He, and isotopic depletion with distance downstream. We estimated total groundwater discharge by inverting a stream transport model against ^{222}Rn and discharge measured in the stream. The salinity, ^{4}He, and stable isotope composition of discharging groundwater was then estimated by fitting modeled values to observed in-stream values. Estimated groundwater inflow to the stream was well within the ranges observed in springs, indicating that the main source of streamflow is deep, regional groundwater. These results show that synoptic surveys of environmental tracers in streams can be used to estimate the isotopic composition and constrain the source of groundwater discharging to streams. Our data provide direct field evidence that deep, regional groundwater discharge can be a significant source of streamflow generation in arid, topographically complex watersheds.

1. Introduction

Groundwater is an important source of streamflow generation, providing baseflow during periods of no precipitation and maintaining water quantity. The recharge source, flow path length, and age of groundwater discharging to the stream control baseflow discharge quantity and quality. Streamflow resilience to changes in climate, land use, and water resource extraction disturbances is a function of streamflow source (e.g. Tague and Grant, 2009). Longer groundwater residence times and flow paths lead to larger stability in baseflow, but increase the total area over which groundwater and stream must be co-managed. Shorter groundwater residence times and flow paths will translate to high variability and susceptibility of baseflow, but decrease the area of management of water resources (Manga, 1996; Gardner et al., 2010; Solder et al., 2016). Additionally, the mean residence time of water through a catchment can exceed the hydrologic pressure

* Corresponding author.
E-mail address: kbeisner@usgs.gov (K.R. Beisner).

https://doi.org/10.1016/j.jhydrol.2018.06.078
Received 12 February 2018; Received in revised form 20 June 2018; Accepted 28 June 2018
Available online 30 June 2018
0022-1694/ Published by Elsevier B.V.

response by orders of magnitude (McDonnell and Beven, 2014; Hrachowitz et al., 2016). Knowing the age and scale of groundwater circulation is critical for predicting streamflow response to climatic and anthropogenic disturbance.

Deep regional groundwater discharge to streams remains one of the least understood portions of the watershed budget. The volume of deep groundwater discharge is important in determining stream response to climatic changes in snowmelt dominated catchments (Tague and Grant, 2009). Genereux et al. (2013) show that regional groundwater is critical for understanding watershed scale nutrient and carbon cycling. The age distribution of groundwater discharging to the stream controls the water quality of baseflow and the migration and discharge of anthropogenic nutrients (Gilmore et al., 2016). The volume of regional groundwater discharge should be known in order to accurately predict watershed quantity and quality.

Regional groundwater has been theoretically shown to be an important component of streamflow generation. Topography, precipitation and geology combine to determine the relative contribution of regional groundwater (Haitjema and Mitchell-Bruker, 2005). Gleeson and Manning (2008) found that the high topography, and low precipitation of the western US, indicate that much of the groundwater discharge to rivers in this area should be dominated by regional groundwater flow. Regional scale coupled surface and groundwater models have shown that mean residence times in streams range from 1 to 10 years in upland catchments, to greater than 10,000 years in larger arid catchments in the western US (Maxwell et al., 2016).

Theoretical studies of regional groundwater contributions to streams have had some initial field verification. Using stream chemistry, regional groundwater flow has been shown to be important in streamflow generation in mountainous areas of Colorado (Frisbee et al., 2011). Gardner et al. (2011) used dissolved ^{4}He and ^{222}Rn measured to calculate the fraction of total groundwater coming from regional groundwater discharge to rivers. This technique has been shown to work in other basins with different geology (Smerdon et al., 2012). By increasing the number of age tracers, which provide information over a broader range of residence times, a more detailed look at the distribution of flow paths can be accomplished (Stolp et al., 2010; Smerdon et al., 2012; Harrington et al., 2013; Solomon et al., 2015).

At the continental scale the majority of active groundwater circulation may be young in age (Gleeson et al., 2015), and the majority of streamflow has a short residence time (Jasechko et al., 2016). However, regional groundwater discharge should be important in arid locations with high topographic relief (Haitjema and Mitchell-Bruker, 2005). These two juxtaposing arguments indicate that the relative role and amount of regional groundwater discharge is an open question in watershed hydrology and field based studies are required to help solve this conundrum. The amount of regional groundwater discharge to rivers has not been quantified by field observation in most hydrogeological settings, including the geologically, hydrologically and topographically complex western US where regional groundwater flow may be a large component.

In this study, we used a comprehensive analytical suite of both physical and chemical indicators of groundwater input to a river. The results of the study were modeled to provide a better understanding of how knowledge of groundwater geochemistry can inform in-stream measurements of groundwater contribution. The results of this study can help inform future investigations as to which analytes are needed for understanding groundwater contribution to surface waters, when a comprehensive analytical suite can not be measured. Specifically this study used synoptic differential stream gaging combined with ^{222}Rn, dissolved noble gases including ^{4}He, stable isotopes of water ($\delta^{18}O$ and $\delta^{2}H$), and stream conductivity to investigate the isotopic composition and thus source of groundwater discharge in a strongly gaining reach of the Verde River. By combining measurements of stream discharge and isotopic composition, we use the stream chemistry to infer groundwater composition and source. This technique allows us to constrain the source location and flow and path length for groundwater discharge and to identify the role of regional groundwater contribution. These results show that stream surveys of discharge, ^{4}He, $\delta^{18}O$ and $\delta^{2}H$, and stream conductivity can be used to identify the role regional groundwater discharge and provide direct evidence of the role of regional discharge in arid, high topography areas.

1.1. Hydrogeologic setting

The Verde River is one of the largest perennial sources of water in Arizona flowing from near Paulden, AZ to the Salt River near Fountain Hills, AZ. A portion of the Verde River, downstream of the study area, is designated as Wild and Scenic (Verde River, Arizona, 2017) and another portion is part of the State Parks system as the Verde River Greenway State Natural Area (Verde River Greenway, 2017). Yavapai County is one of the fastest growing rural counties in the United States (Blasch et al., 2006). Increased population growth will result in increased demand on the region's water resources (Blasch et al., 2006) and a better understanding of the system is needed to understand the possible effects to the Verde River. Better knowledge of the location of groundwater contributions to the river are also needed to refine groundwater models of the area to understand impacts from future changes to the groundwater system.

Using discharge measurements on a broad scale throughout the middle Verde River, Blasch et al. (2006) and Bills et al. (2007) found a large increase in discharge near a bend in the river known as Mormon Pocket (Fig. 1). The study described herein focuses on the area of the Verde River from Mormon Pocket to the USGS Verde River near Clarkdale streamgage (hereafter referred to as the USGS Clarkdale gage, Fig. 1).

The stratigraphic section in the study area consists of a sequence of Cambrian to Permian sedimentary rocks overlain by Tertiary volcanic rocks and younger alluvial sedimentary deposits. The Mississippian Redwall Limestone is the dominant lithology at the upper and lower ends of Mormon Pocket with the Supai Group cropping out at the Verde River between, due to dip of 5 to 10 degrees to the northeast of the beds in the area (Lehner, 1958, Fig. 2). A fault cuts across the Verde River on the east side of the bend in the Verde River near Mormon Pocket (Fig. 1; Lehner, 1958), but there are no mapped structural features within Mormon Pocket on the map from DeWitt et al. (2008). The Railroad Fault splits just north of the Verde River and rock units are displaced along the fault where the Verde River crosses the fault expression (DeWitt et al., 2008). The Railroad Fault displaces the Devonian Martin Formation and Cambrian Tapeats Sandstone to the course of the Verde River upstream of the confluence with Sycamore Creek. The USGS Clarkdale gage is located just upstream of Tertiary alkali basalt deposits forming a steep canyon through which the Verde River flows.

The Redwall Limestone is a regional aquifer in the area and there are some springs discharging from the Supai Group near the Grand Canyon to the north of the study area. Two springs entering the Verde River at the upper side of Mormon Pocket are discharging from the Redwall Limestone and one discharges from the Supai Group within Mormon Pocket. Another spring enters the Verde River from the Supai Group just upstream of the USGS Clarkdale gage. In Sycamore Canyon, Sycamore Creek begins perennial flow at Parsons Spring and then gains flow from Summers Spring, which discharges from the Redwall Limestone near a fault expression.

The study area is located in a semidesert grassland and surrounded by Great Basin conifer woodland biotic communities (HabiMap Arizona, 2018). Annual precipitation varies from around 25–38 cm in the basins to around 51–101 cm at the crest of the mountains (Blasch et al., 2006). Precipitation primarily occurs in two seasons, summer monsoon characterized by short lived, intense and localized convective rainstorms (July through September) and the other characterized by longer lived, less intense and more regional frontal precipitation events (December through March). June is typically a month with low

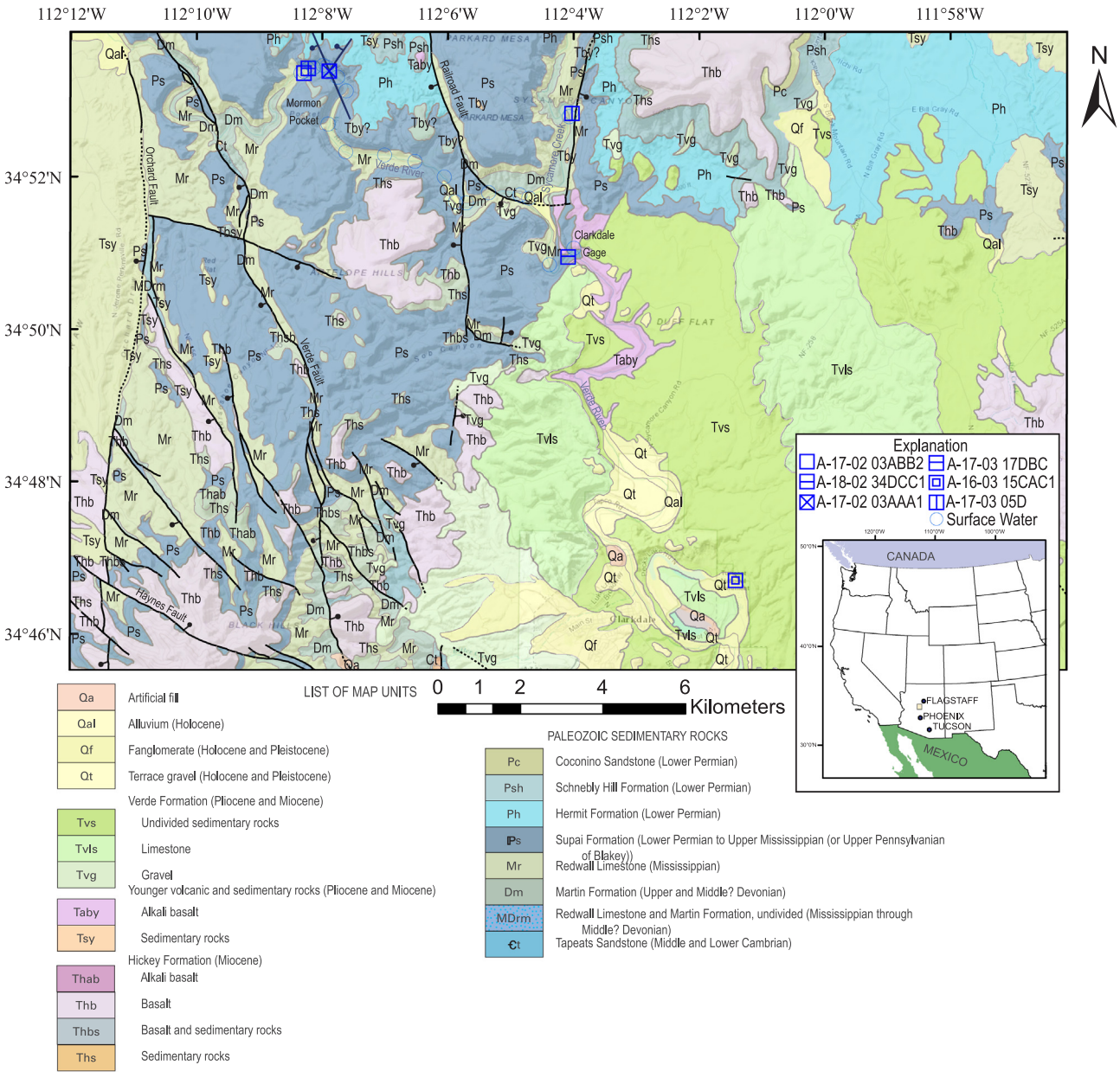

Fig. 1. Map of study area with sample sites and inset graph of location in United States. Geology from DeWitt et al. (2008).

precipitation in central Arizona, occurring prior to the summer monsoon rain. Flow in the Verde River during June represents primarily baseflow conditions (Fig. 3a). The USGS Clarkdale gage has been monitored since 1916, with continuous mean monthly data since 1965, and mean monthly streamflow in June was the lowest (1.67 m^3/s) on record in 2016 (Fig. 3b).

2. Materials and methods

2.1. Field

Water samples were collected following standard U.S. Geological Survey protocols (U.S. Geological Survey, variously dated). Field parameters including pH, water temperature, specific conductance, dissolved oxygen, and barometric pressure were measured in the center of the river and at each spring site just before the water sample was collected. Water samples were filtered (0.45 µm) for major cations, trace, alkalinity, carbon-14, strontium isotopes, and all, except for the major anions, alkalinity and carbon-14 samples, were preserved to pH < 2 by using ultrapure nitric acid. Unfiltered samples were collected for tritium, and $\delta^{18}O$ and $\delta^{2}H$. Alkalinity titrations using the incremental equivalence method were performed within 5 h of sample collection (U.S. Geological Survey, variously dated). Discharge measurements were made using the midsection method with a Flowtracker ADV (Turnipseed and Sauer, 2010). Measurements were considered good ratings with an estimated 5 percent error.

^{222}Rn samples were collected using a glass syringe and needle. Then 10 mL was discharged from the needle beneath 10 mL mineral oil cocktail solution in a scintillation vial according to methods in the U.S. Geological Survey National Field Manual (U.S. Geological Survey, variously dated). Noble gas samples were collected in copper tubes (2 per sample) which were sealed with refrigerator clamps (Weiss, 1968).

2.2. Analytical

Stable isotope ratios ($\delta^{18}O$ and $\delta^{2}H$) were measured at the U.S. Geological Survey Reston Stable Isotope Laboratory using mass spectrometry following methods by Révész and Coplen (2008a,b), the 2-

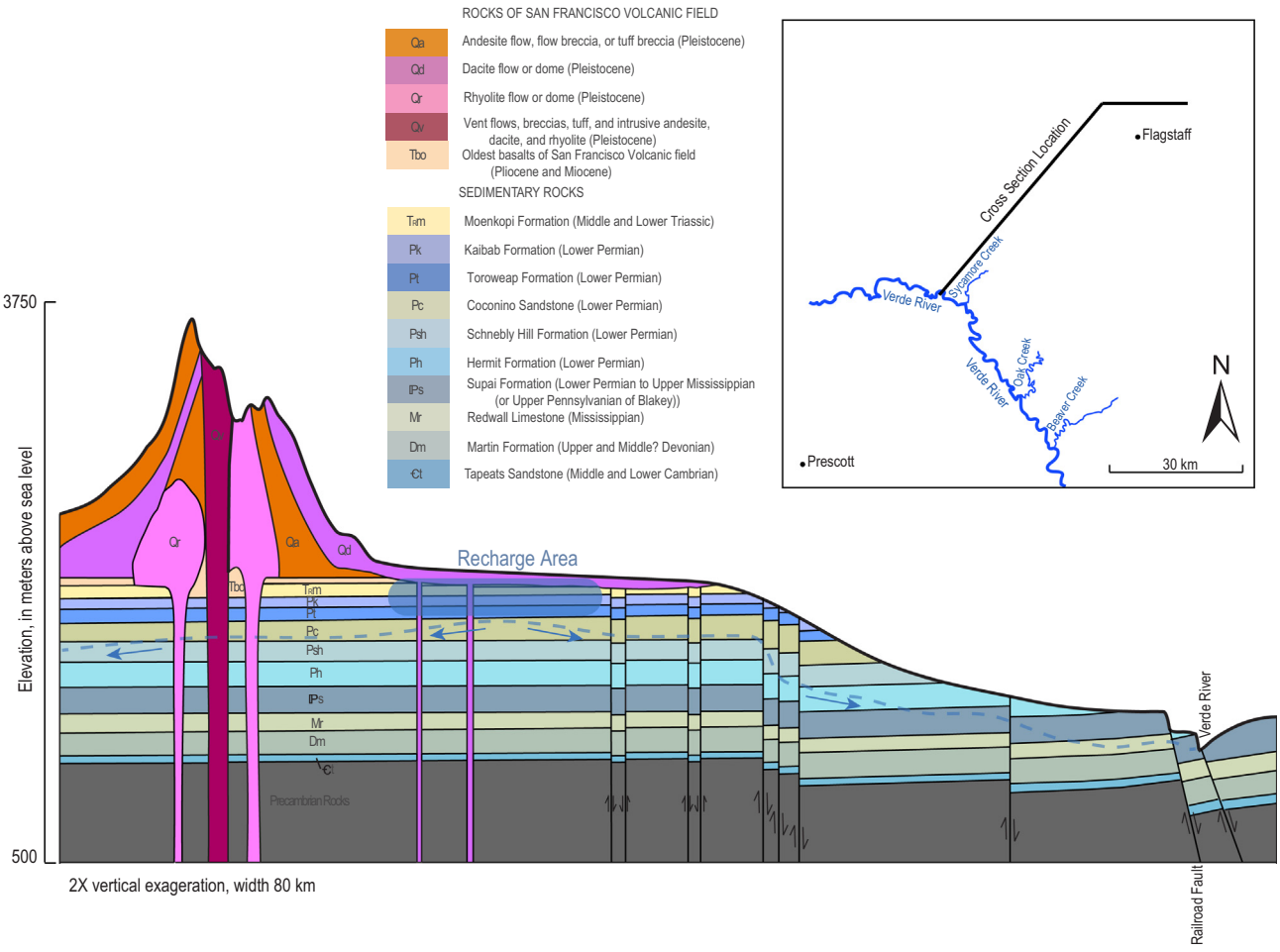

Fig. 2. Conceptual model cross section of the geology and hydrology between Flagstaff and the Verde River at Mormon Pocket, modified from Lehner (1958), Ulrich et al. (1984), and Blasch et al. (2006).

sigma uncertainties are 0.2‰ for oxygen and 2‰ for hydrogen isotopic ratios reported relative to Vienna Standard Mean Ocean Water. Strontium isotope ratios ($^{87}Sr/^{86}Sr$) were measured by the U.S. Geological Survey National Research Program Laboratory in Menlo Park, California by using multi-collector mass spectrometry following methods described in Bullen et al. (1996) and are precise to 0.00002 or better at the 95% confidence level.

^{222}Rn was analyzed by liquid scintillation methods at the U.S. Geological Survey National Water Quality Laboratory using method ASTM D 5072-98 (ASTM, 2016). The laboratory reporting level was 20 pCi/L, and some values were reported below 20 pCi/L on a sample-specific critical level basis. Three replicate samples of ^{222}Rn were collected to determine the variability of the results.

Noble gases (He, Ne, Ar, Kr, and Xe) were analyzed by the U.S. Geological Survey Noble Gas Laboratory (Hunt, 2015). Tritium was measured at the USGS Noble Gas Laboratory by He ingrowth methods for samples collected in 2014 and 2015 (Bayer et al., 1989). Tritium, carbon-14, and carbon-13/12 were analyzed at the University of Arizona Accelerator Mass Spectrometry Laboratory in 2011. Carbon-14 and carbon-13/12 were analyzed by the National Ocean Sciences Accelerator Mass Spectrometry (NOSAMS) at Woods Hole Oceanographic Institution for sample collected in 2014.

2.3. Stream transport modeling

We modeled stream discharge and solute concentration using a numerical solution of the coupled mass balance equations for streamflow and stream solute concentration. The mass balance equation for fluid flow along the reach is given by:

$$\frac{\partial Q}{\partial x} = \frac{Q_{tr}}{\partial x} + P \cdot w - E \cdot w + q_{gi} \cdot w + q_{go} \cdot w - \frac{Q_p}{\partial x} \quad (1)$$

where Q is the stream discharge (m^3/s), x is the discretized distance downstream (m), Q_{tr} is spatially distributed location of tributary discharge (m^3/s), P is the precipitation rate (m/s), E is the evaporation rate (m/s), q_{gi} is the groundwater discharge gain flux (m/s), q_{go} is the groundwater loss flux (m/s), Q_p is the spatially distributed locations of stream diversion (m^3/s) and w is the stream width (m).

For 1-d advective- dispersive transport in the stream, with groundwater inflow, atmospheric gas exchange and first order solute decay, mass balance gives:

$$\frac{\partial C}{\partial x} = \frac{\partial}{\partial x}\left(\frac{D \cdot A}{Q}\frac{\partial C}{\partial x}\right) + \frac{q_{gi} \cdot w}{Q} \cdot C_{gw} - \frac{q_{go} \cdot w}{Q} \cdot C - \frac{k \cdot w}{Q}(C - C_{atm}) - \frac{A}{Q}\lambda C + \frac{1}{Q}\frac{Q_{tr}}{\partial x} \cdot C_{tr} - \frac{1}{Q}\frac{Q_p}{\partial x} \cdot C \quad (2)$$

where C is the stream concentration (mol/m^3), D is the longitudinal hydrodynamic dispersivity (m^2/s), A is the stream cross-sectional area (m^2), C_{gw} is the local groundwater concentration (mol/m^3), k is the gas exchange velocity (m/s), C_{atm} is the atmospheric equilibrium concentration of the tracer (mol/m^3), λ is the decay coefficient (s^{-1}), C_{tr} is the concentration of the tributary at the confluence (mol/m^3), and all other variables have been defined for Eq. (1).

2.3.1. Solution technique

Eqs. (1) and (2) are a set of partial differential equation, which are

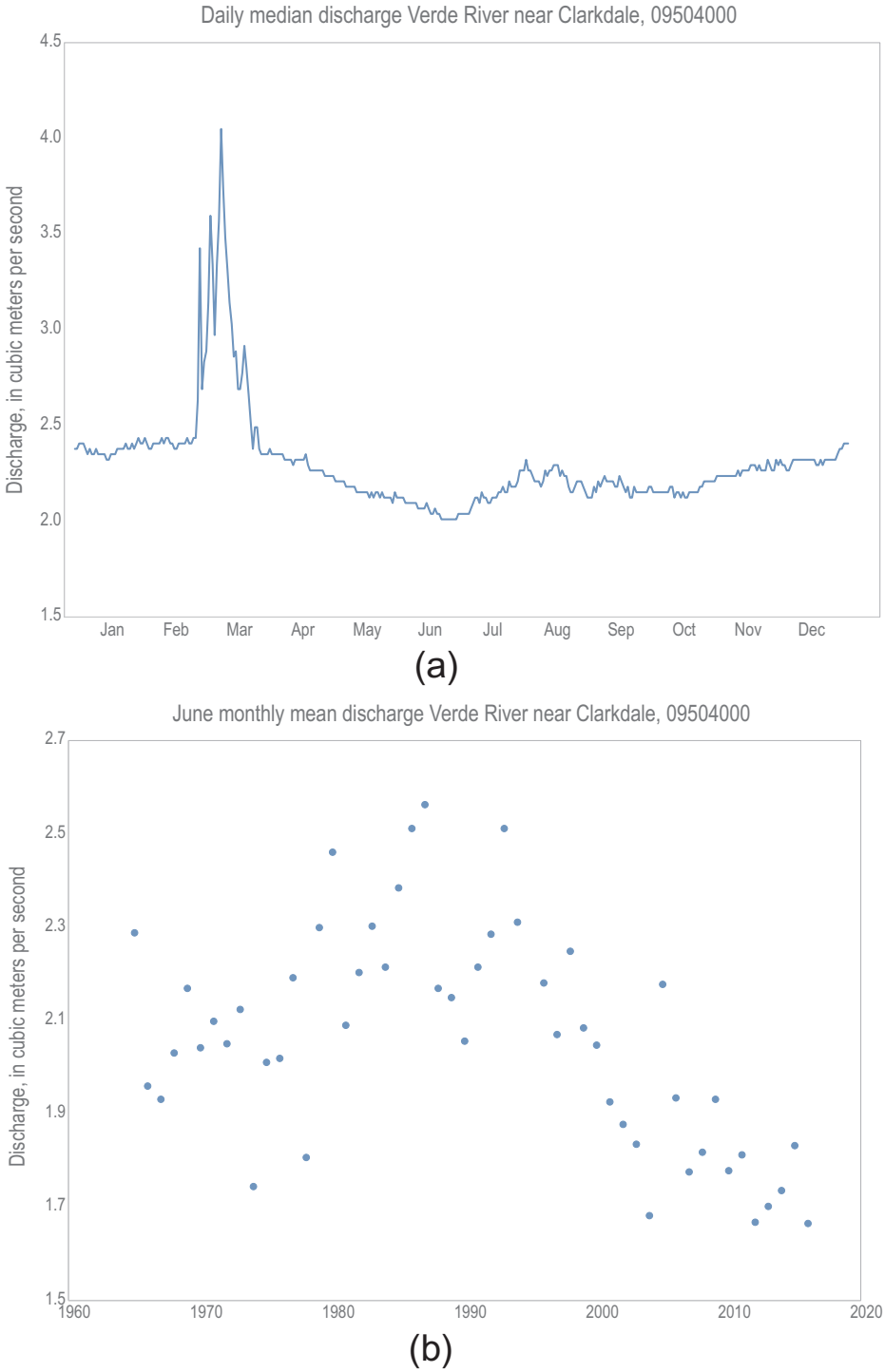

Fig. 3. (a) Daily median discharge from 1966 to 2016 for the USGS Verde River near Clarkdale gage (b) Mean monthly June discharge at USGS Verde River at Clarkdale gage.

coupled through the discharge and stream geometry. We solve these equations using a fully implicit, finite volume method based on FiPy, a python finite volume solver library (Guyer et al., 2009). For a forward run, we solve Eq. (1) for the discharge along the stream reach (Q) given the spatially distributed amount of groundwater gain and loss, stream geometry, the stream tributary and diversion discharges, precipitation and evaporation rates. We then solve Eq. (2) for the stream concentration profile of each tracer, given the concentration of tracers measured in groundwater flow along the reach, and the tracer dependent gas exchange velocity, decay coefficient and the atmospheric equilibrium concentration.

2.3.2. Boundary conditions

The stream reach is discretized from the upstream to downstream extents of the study. For this study, the total reach length investigated was 11.3 km. The reach is discretized at roughly 1 m grid spacing. Constant discharge and constant concentration, Dirichlet boundary conditions, set to the measured discharge and concentration at the upstream sampling site are implemented at the upstream end of the stream transport model. Constant concentration gradient (Neumann),

and constant discharge (Diriclet) boundary conditions are set at the bottom end of the reach.

Atmospheric equilibration is only active for dissolved gases, where the gas exchange coefficient is greater than zero. Atmospheric equilibrium concentration of dissolved noble gases in water (ccSTP/g) was calculated using:

$$C_i = \frac{(x_a \cdot P)_i}{K_h(T)}\left(\frac{V_m}{M_{h2o}}\right) \quad (3)$$

Given the known atmospheric concentration (x_z - mixing ratio), the Henry's coefficient $K_h(T)$in (GPa) and stream temperature (T) in degrees C, atmospheric pressure Pin GPa, the standard molar volume $V_m$and the molar mass of water M_{h2o}. T was set as the average temperature for all sampling times, atmospheric pressure was estimated from a standard atmospheric adiabatic lapse rate curve and the average elevation of the reach. The gas-dependent Henry's coefficient was calculated for the measured stream temperature using Henry's coefficient relationships summarized in Ballentine et al. (2002). For non-volatile tracers, the gas exchange coefficient and atmospheric equilibrium gas concentrations are both set to zero, which removes the gas exchange terms from Eq. (2).

2.3.3. Parameterization

Parameters were chosen to represent characteristic site conditions at the time of the synoptic survey. Atmospheric equilibrium concentration for ^{4}He was calculated using the Henry's coefficient at the given air temperature from Ballentine et al. (2002). For ^{222}Rn, the atmospheric equilibrium concentration was set to zero. Atmospheric ^{4}He was set to the standard atmospheric concentration at 1100 m elevation and 21 degrees Celsius of 4E−8 ccSTP/g. All other tracers are assumed to be non-volatile and not exchange with the atmosphere over the reach length. Longitudinal dispersivity was set to zero, which means that numerical dispersion with dispersivity of the grid cell spacing (~1 m) controls the dispersive flux given our fully implicit solution technique. The only decaying tracer simulated is ^{222}Rn, for which a decay coefficient of 3.82 d^{-1} was assigned (Cook and Herczeg, 2000). Stream widths and average depths were measured at each discharge measurement cross section then were linearly interpolated along the stream profile between measurement locations for the model (Fig. 4). Stream cross sectional area along the model domain was then calculated as the width times the average depth. We estimate the gas exchange coefficient for ^{4}He and ^{222}Rn using stream hydraulics and temperature after Raymond et al. (2012) and references therein. First we calculate the k_{600} gas exchange velocity, which is the gas exchange velocity for a Schmidt number of 600 (CO_2 at 20 °C), using the average slope (S), velocity (V), and depth (D) in Eq. (4):

$$k_{600} = 5037(VS)^{0.89}D^{0.54} \quad (4)$$

The gas specific exchange velocity is then found by calculating the Schmidt number (Sc) for the gas of interest at the stream temperature and using the relationship in Eq. (5) (Raymond et al., 2012):

$$\frac{k_{g1}}{k_{600}} = \left(\frac{Sc_{g1}}{600}\right)^{-\left(\frac{1}{2}\right)} \quad (5)$$

We estimate a gas exchange velocity of 4.7 m/d for ^{222}Rn and 11.4 m/d for ^{4}He (Table 1).

2.3.4. Modeling strategy

We estimate the average groundwater discharge to the stream in over 1 km steps in the following manner. Groundwater discharge was assumed to follow as a step function, with a 1 km step length. Groundwater concentrations of tracers were measured in springs at several sites along the reach. We assume that all groundwater discharge has reached secular equilibrium and is equal to the concentration sampled in springs along the river. The concentration of ^{222}Rn in the groundwater for each inflow step was assigned along the model profile by the nearest neighbor of sampled groundwater. We then estimate the total groundwater inflow along the reach by fitting our stream transport model to the observations of stream discharge and ^{222}Rn concentration in the stream using a Marquart-Levenberg optimization routine which minimized the chi squared residual between model and observed ^{222}Rn and stream discharge. Using the estimated distributed groundwater discharge, the concentration of ^{4}He, stable isotopes, and conductivity in the discharging groundwater was then estimated by fitting the observed stream concentration of these tracers. The estimated isotopic concentrations can then be compared to those measured in springs and the isotopic signature used to assess whether a regional source similar to that feeding springs in the area is the dominant source of groundwater flow to the stream.

3. Results and discussion

The location of the sample sites in this study are presented in Table 2.

3.1. Geochemistry of contributing springs

General chemistry of the groundwater sites in this study are circumneutral pH (6.8–7.9), water temperature ranging from 18.2 to 21.2 degrees Celsius, low specific conductance (318–555 μS/cm), and dissolved oxygen ranging from 6.4 to 7.5 mg/L. The three sampled springs discharging in Mormon Pocket were on the lower end of the range of specific conductance (318–375 μS/cm) and temperature (18.2–18.7 degrees Celsius). The dominant water type is calcium-bicarbonate (Fig. 5).

The majority of the groundwater sites had stable isotope values ranging from −11.9 to −11.59 per mil and −83.4 to −81.1 per mil for δ^{18}O and δ^2H respectively (Fig. 6). All of the samples plotted between the local meteoric water lines (LMWL) for the Verde River watershed from Blasch et al. (2006) (determined from precipitation in Flagstaff between 1962 and 1974) and Beisner et al. (2016) (determined from precipitation between 2003 and 2014).

Recharge elevation from stable isotope values can be calculated using Eqs. (6) and (7) from Beisner et al. (2016), converted to represent elevation in meters presented here as Eqs. (6) and (7). Equations were determined empirically from precipitation collectors throughout the Verde River watershed over a period of 10 years, it does not account for evaporation prior to recharge.

$$\delta^{18}O = -0.001312z - 8.87 \quad (6)$$

$$\delta^2H = -0.009514z - 59.8 \quad (7)$$

where z represents the recharge elevation in meters. The range of recharge elevation for the group of spring samples contributing groundwater to the study area (−11.59 to −11.9 and −81.1 to −83.4 per mil for δ^{18}O and δ^2H respectively) ranges from 2073 to 2309 m for δ^{18}O and 2239 to 2480 m for δ^2H (table 3). The elevation of the uppermost Verde River sample from Mormon Pocket from this study is 1120 m and the lowest elevation is from the USGS Clarkdale gage at 1067 m.

Noble gas samples were collected from groundwater samples and represent a more direct measurement of recharge temperature and elevation. ^{4}He concentrations in groundwater samples ranged from 4.1E to 6 to 8.2E−7 cc/g of water at standard temperature and pressure (STP). ^{222}Rn concentration in the groundwater samples ranged from 92 to 440 pCi/L. Recharge temperature and elevation were calculated using Ne, Ar, Kr, and Xe (Table 3) with the closed system equilibration model (CE) (Aeschbach-Hertig et al., 2000) using a standard inverse technique (Newton method) to minimize the error-weighted misfit (χ^2) between measured and modeled values (Aeschbach-Hertig et al., 1999; Ballentine and Hall, 1999; Manning and Solomon, 2003).

A local relationship between recharge temperature and elevation

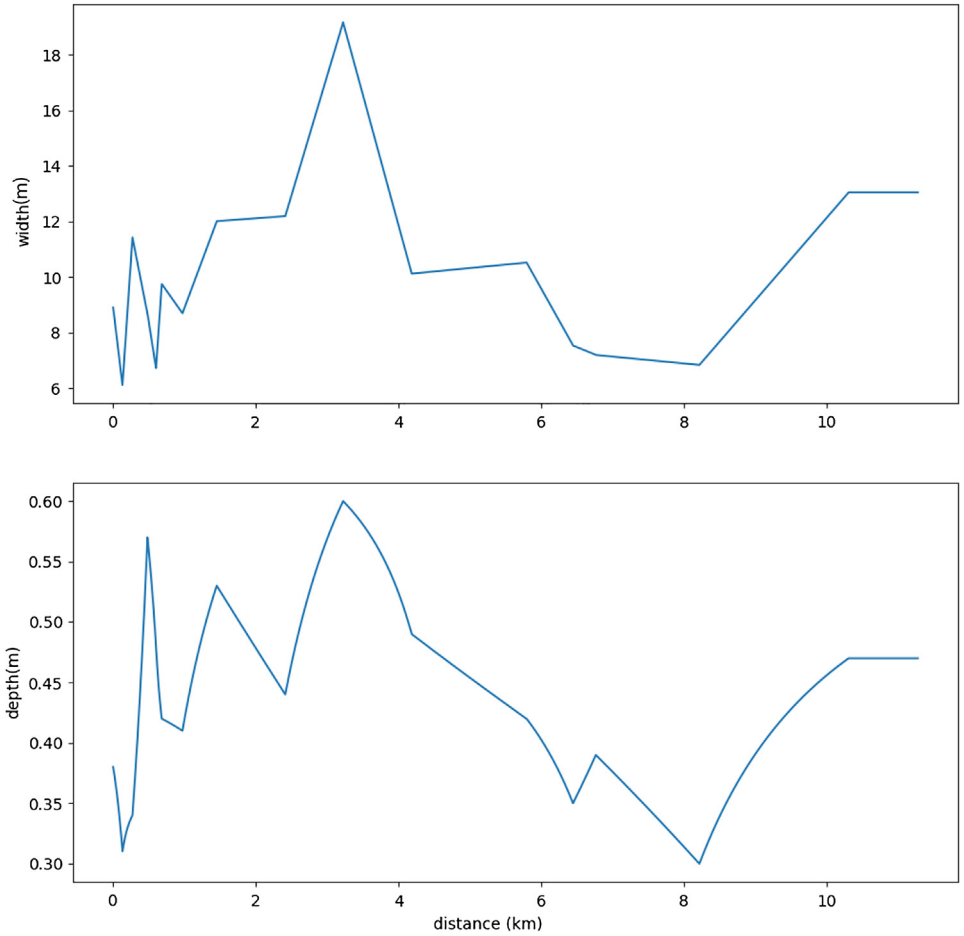

Fig. 4. Interpolated stream width and depth along the reach.

Table 1
Model parameters.

Parameter	Description	Value	Note
P	Precipitation (m/s)	0	field conditions
E	Evaporation (m/s)	1.23×10^{-7}	average June pan evaporation for the area
W	stream width (m)	Fig. 3	stream discharge measurements
A	stream cross section area (m^2)	w * d	stream discharge measurements
D	dispersion coefficient (m^2/s)	0	will be equal to grid spacing for fully implicit solution
K	gas exchange velocity (m/d)	4.7, 11.4[5]	Rn, He – Gardner et al. (2011)
λ	decay coefficient (s-1)	4.43×10^{-5}	Cook and Herczeg (2000)

can place useful constraints on recharge elevation (Zuber et al., 1995; Aeschbach-Hertig et al., 1999; Manning and Solomon, 2003). A temperature lapse rate (Ta) was calculated for the Verde River watershed (presented in Eq. (8)) using mean annual air temperature from available weather stations located at different elevations with a decrease of 8.1 degrees Celsius per 1000 m (Fig. 7), which is similar to the slope of 8.7 degrees Celsius per 1000 m from Johnson et al., (2012) from the Verde River watershed.

$$Ta = -0.0081z + 25.432 \quad (8)$$

where Ta represents the recharge temperature in degrees Celsius and z represents the recharge elevation in meters. Water table temperatures, and thus recharge temperatures, for typical depths below ground surface of 5–50 m are generally 0–3 degrees Celsius above Ta (Domenico and Schwartz 1990; Lee and Hahn 2006; Cey 2009). Maximum and minimum noble gas recharge temperatures were computed for each groundwater sample, where the minimum value is the spring discharge elevation and the maximum is 2400 m.

Data indicate that the groundwater samples recharged from cooler temperatures and higher elevations from where they discharge near the Verde River. Recharge temperatures ranged from 11.1 to 14.4 degrees Celsius and elevations from 1550 to 1850 m using the closed system equilibrium model (Aeschbach-Hertig et al., 2000) for the three springs discharging in Mormon Pocket (A-17-02 03AAB2, A-18-02 34DCC1 and A-17-02 03AAA1) (Fig. 7).

Recharge elevations determined from noble gas and stable isotope data provides a valuable opportunity to compare recharge elevations calculated by each method, which are presented in Table 3. Recharge elevations determined from δ^2H were the highest. Stable isotope recharge elevations were determined from empirical data collected from recent precipitation (Beisner et al., 2016), which may not be representative of groundwater recharge during past climate conditions. The fit of the noble gas data to the model used to calculate recharge parameters can be effected by degassing prior or during sample collection.

Two of the springs were sampled previously for carbon-14 and tritium and contain old water datable by radiocarbon methods: Shea Spring (30.1 pmc, corrected age 2211 to 5069 years before present; Beisner et al., 2014) and Summers Spring (35.1 pmc, corrected age 4600 years before present; Bills et al., 2007). Shea Spring tritium value was below the laboratory reporting level (< 1.1 TU in 2011; Beisner et al., 2014) and Summers Spring tritium value was above the

Table 2
Sample names and locations (datum is NAD83).

USGS Site ID	Station Name	Decimal Latitude	Decimal Longitude	Sample Type
345324112082000	VERDE RIVER AT MORMON POCKET	34.8900	−112.1389	River
345325112081702	VERDE RIVER 0.12 MI DOWNSTREAM OF RAFAEL DRAW	34.8903	−112.1382	River
345327112081301	VERDE RIVER 0.21 MI DOWNSTREAM OF RAFAEL DRAW	34.8909	−112.1371	River
345329112080801	VERDE RIVER 0.34 MI DOWNSTREAM OF RAFAEL DRAW	34.8913	−112.1355	River
345330112075901	VERDE RIVER 0.5 MI DOWNSTREAM OF RAFAEL DRAW	34.8917	−112.1331	River
345329112075601	VERDE RIVER 0.58 MI DOWNSTREAM OF RAFAEL DRAW	34.8913	−112.1321	River
345326112075401	VERDE RIVER 0.65 MI DOWNSTREAM OF RAFAEL DRAW	34.8907	−112.1316	River
345216112074901	VERDE RIVER BLW MORMON POCKET	34.8789	−112.1316	River
345321112074501	VERDE RIVER NEAR BM 3675	34.8891	−112.1291	River
345310112073701	VERDE RIVER 500 YARDS BELOW BM 3675	34.8861	−112.1268	River
345222112073601	VERDE RIVER 1.5 MI UPSTREAM OF RAILROAD DRAW	34.8728	−112.1268	River
345220112065901	VERDE RIVER 0.8 MI UPSTREAM OF RAILROAD DRAW	34.8722	−112.1164	River
345215112063001	VERDE RIVER 0.2 MI UPSTREAM OF RAILROAD DRAW	34.8709	−112.1084	River
345203112060201	VERDE RIVER 0.4 MI DOWNSTREAM OF RAILROAD DRAW	34.8675	−112.1006	River
345144112055101	VERDE RIVER 0.9 MI DOWNSTREAM OF RAILROAD DRAW	34.8622	−112.0975	River
345143112054101	VERDE RIVER 1.2 MI UPSTREAM OF SYCAMORE CREEK	34.8620	−112.0946	River
345151112051700	VERDE RIVER 0.6 MI ABOVE SYCAMORE CREEK	34.8642	−112.0888	River
345150112045001	VERDE RIVER 250 YARDS ABOVE SYCAMORE CREEK	34.8638	−112.0804	River
345147112044101	SYCAMORE CREEK 10 YARDS ABOVE VERDE RIVER	34.8631	−112.0781	River
345055112042101	VERDE RIVER 1.4 MI DOWNSTREAM OF SYCAMORE CREEK	34.8487	−112.0725	River
345252112040301	SYCAMORE CREEK NEAR SUMMERS SPRING	34.8810	−112.0676	River
345255112035900	SYCAMORE CREEK UPSTREAM FROM SUMMERS SPRING	34.8820	−112.0671	River
09504000	VERDE RIVER NEAR CLARKDALE, AZ	34.8522	−112.0660	River
345325112081701	A-17-02 03ABB2	34.8903	−112.1381	Spring
345328112081401	A-18-02 34DCC1	34.8911	−112.1371	Spring
345327112075301	A-17-02 03AAA1	34.8907	−112.1315	Spring
345102112040001	A-17-03 17DBC	34.8506	−112.0674	Spring
345255112035801	A-17-03 05D (Summers Spring)	34.8820	−112.0668	Spring
344648112012000	A-16-03 15CAC1 (Shea Spring)	34.7800	−112.0222	Spring

laboratory reporting level at 1.1 TU in 2003 (Bills et al., 2007) and 1.5 TU in 2011.

Strontium isotopic ratio in groundwater samples collected during this study ranged from 0.70664 to 0.70739 (Fig. 8). Groundwater samples from springs in Mormon Pocket had lower strontium isotopic values (0.70664–0.70677) compared with the groundwater at Summers Spring (Bills et al., 2007) and Shea Spring (0.7073–0.7077) (Fig. 8). Tertiary volcanic rocks including basalt have the lowest measured strontium isotopic values (0.70463–0.70535; Bills et al., 2007), Paleozoic sedimentary rocks have intermediate strontium isotopic values (0.70756–0.70930; Bills et al., 2007) and Precambrian igneous rocks had the most radiogenic values (0.71618–0.76912; Bills et al., 2007). Precipitation values have been reported to range from 0.7098 to 0.7107 (Frost and Toner, 2004).

Groundwater from the western Flagstaff area have low strontium isotopic values (0.70588–0.70655; Bills et al., 2007) and 0.7055 from groundwater near Stoneman Lake (Johnson et al., 2012), which may reflect interaction with Tertiary volcanic rocks. Groundwater from springs in Mormon Pocket values are between the Paleozoic sedimentary rock that the springs discharge from and the tertiary volcanic values and may suggest a component of water interacting primarily with volcanic rock and some interaction with Paleozoic sedimentary rocks (Fig. 2).

3.2. Seepage analysis

3.2.1. Discharge

Streamflow in late June 2016 increased from 0.57 m^3/s to 1.27 m^3/s within approximately 1.4 km as the Verde River flows through Mormon Pocket (Fig. 9). There are three distinct visible spring discharge locations in this reach that contribute to increases in flow, but their combined flow of 0.21 m^3/s does not account for all of the discharge increase of 0.7 m^3/s. There appear to be other locations of diffuse groundwater input to the Verde River in this reach. Downstream of Mormon Pocket, the river gains 0.15 m^3/s in the next 5 km to a total flow value of 1.42 m^3/s. The Verde River gains approximately 0.18 m^3/s from Sycamore Creek 8.4 km downstream of the beginning of the study reach in Mormon Pocket. The flow at the USGS Clarkdale gage downstream of Sycamore Creek was 1.68–1.71 m^3/s on 6–29-2016 and indicates there may be 0.1–0.13 m^3/s input of flow between the inflow from Sycamore Creek and the USGS Clarkdale gage. There was one small spring inflow observed just upstream of the USGS Clarkdale gage, but not enough to account for the discharge difference alone.

The discharge at the USGS Clarkdale gage fluctuated daily during the June 2016 investigation on the order of 0.03 m^3/s (Fig. 10). A small discharge peak was observed at the USGS Clarkdale gage starting late 6-29-2016, which rose 0.86 m^3/s over a period of 2 h and 15 min. The peak receded 0.8 m^3/s in 8 h and 30 min to a value 0.06 m^3/s greater than the value before the peak. The peak was not recorded at the USGS Verde River at Paulden gage and indicates that the inflow occurred from tributaries between the two gages. The majority of the 2016 samples (15 out of 20) and discharge measurements (13 out of 14) were collected before the peak.

3.2.2. Radon and Helium

^{222}Rn of in surface water indicates the nearby input of groundwater with large concentrations of ^{222}Rn. ^{222}Rn samples were collected at discharge measurement locations and additional sites to obtain a good spatial coverage of data. Replicate samples of ^{222}Rn showed good agreement; 1% (with a 2 pCi/L difference), 2% (with a 2 pCi/L difference), and 30% (with a 16.3 pCi/L difference).

^{222}Rn was measured at all but one of the surface water sites and ^{4}He was measured on a subset of the surface water samples collected in June 2016. ^{222}Rn concentrations in June 2016 were below the laboratory reporting level and ^{4}He concentration was similar to atmospheric concentration (4E − 8 ccSTP/g) in the Verde River at the most upstream site in Mormon Pocket (5.3E − 8 ccSTP/g) (Fig. 12). Downstream of the uppermost site is a small spring input from the right bank and the next downstream Verde River sample had a ^{4}He concentration of 8.6E − 8 ccSTP/g, double the atmospheric equilibrium and associated with an increase of ^{222}Rn to 46 pCi/L (Fig. 12). ^{222}Rn concentration decreased to 77 pCi/L about 0.1 km downstream of the previous site following a

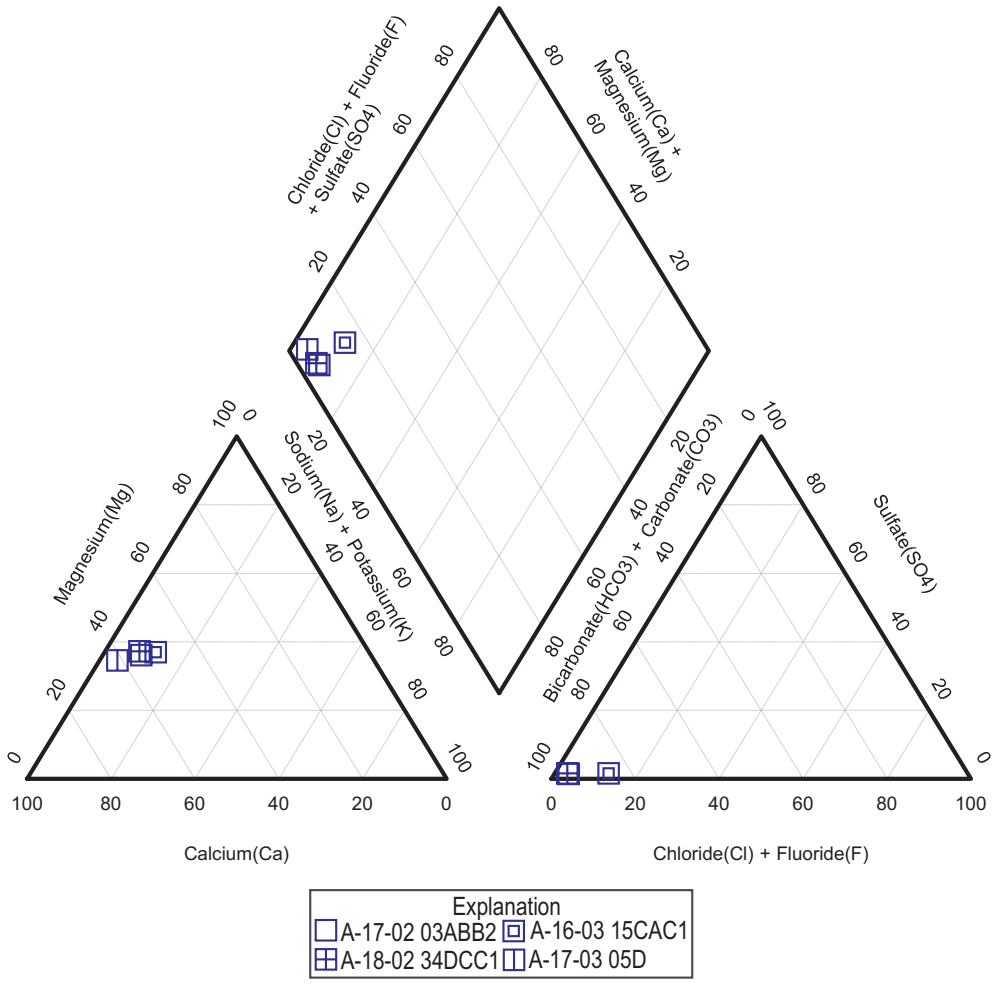

Fig. 5. Piper plot of groundwater samples.

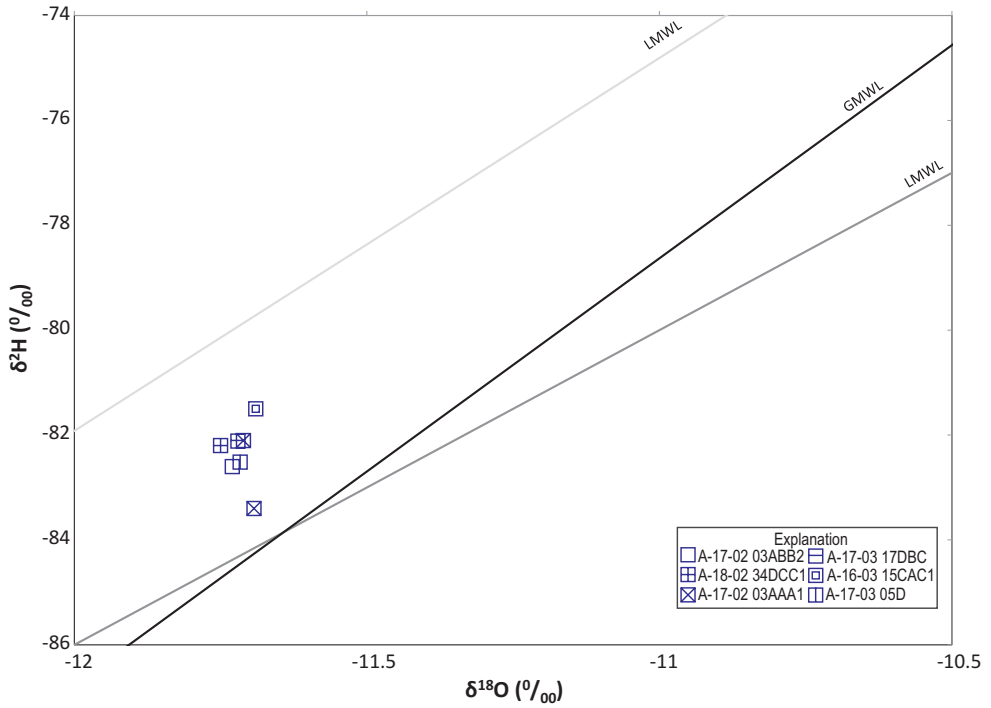

Fig. 6. Stable isotope graph of groundwater samples. The global meteoric water line (GMWL) is from Craig, 1961, the light gray local meteoric water line (LMWL) is from Beisner et al., 2016, and the dark gray LMWL is from Blasch et al., 2006.

Table 3
Recharge parameters computed from dissolved gas and stable isotope data $\delta^{18}O$ and $\delta^{2}H$ elevations determined from Eqs. (6) and (7) derived from Beisner et al. (2016); CE, closed system equilibration model used to determine noble gas recharge parameters and the local recharge temperature lapse rate from Eq. (8); NGRT, noble gas recharge elevation; Ae, initial excess air concentration; F, fraction of excess air loss, χ^2 threshold at the p 0.05 level is 3.84.

Sample	Spring Elevation (m)	Recharge Elevation (m)			NGRT (Ta + 1.5) (°C)	NGRT error (°C)	Ae (ccSTP/g)	F	Model Misfit (χ^2)	R/Ra
		$\delta^{18}O$	$\delta^{2}H$	Noble Gas (Ta + 1.5)						
A-16-03 15CAC1	1015	2149	2281	2400	7.7	0.58	0.001	0	2.53	0.284
A-17-03 05D	1103	2172	2386	2350	8.1	0.57	0.0007	0	3.85	0.230
A-17-03 17DBC	1082	2172	2344	1350	16	1.25	0.1674	0.970	4.29	0.234
A-17-02 03ABB2	1131	2180	2396	1700	13	1.27	0.2920	0.952	1.77	0.295
A-17-02 03AAA1	1116	2165	2344	1850	11.9	0.86	0.1339	0.965	4.61	0.260
A-18-02 34DCC1	1120	2195	2354	1550	14.4	0.75	0.0010	0	0.43	0.294

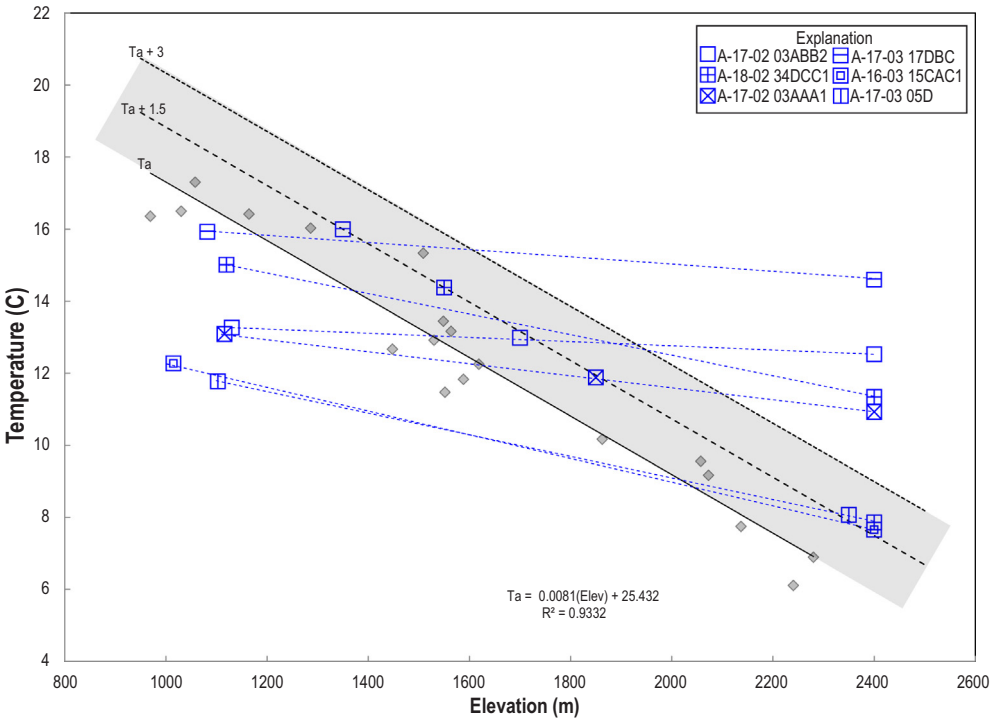

Fig. 7. Noble gas recharge elevation graph. Ta represents mean annual air temperature versus elevation determined from a regression of temperature data from the area depicted by gray diamonds.

stretch of riffle flow with whitewater where there may be some mixture with air and possible loss of ^{222}Rn. ^{4}He concentration in the Verde River downstream of visible seepage of presumed groundwater from the left bank near 1 km downstream was 3.8E−7 ccSTP/g, an order of magnitude greater compared with the uppermost sample and ^{222}Rn increased to a value of 107 pCi/L (Fig. 11). The ^{4}He concentration in the river decreased to 8.7E−8 ccSTP/g at 6.4 km downstream of the uppermost sample, just above the crossing with the Railroad Fault, where ^{222}Rn is also less than the laboratory reporting level (Fig. 12). Downstream of the fault two continuous spatial samples had ^{222}Rn values of 13.2 and 13.1 pCi/L indicating the potential input of groundwater unresolvable within the error of the discharge measurements and the ^{4}He concentration was also slightly higher at 7.5E−8 ccSTP/g. These low level values are below the laboratory reporting level of 20 pCi/L, but were determined by the laboratory to represent a quantifiable concentration.

^{222}Rn concentrations in the Verde River above the confluence with Sycamore Creek were below the laboratory reporting level as was Sycamore Creek just before entering the Verde River. Summers Spring, which contributes almost half of the water to Sycamore Creek, had a ^{4}He concentration of 4.1E−6 ccSTP/g, and most of the ^{4}He had left the water in Sycamore Creek (8.0E−8 ccSTP/g in 2015) and ^{222}Rn was less than the laboratory reporting level just before the confluence with the Verde River (Fig. 12). The Verde River at the USGS Clarkdale gage had a ^{222}Rn value of 28.5 pCi/L, which may indicate the presence of groundwater input to the river downstream of the confluence with Sycamore Creek. Increases of ^{222}Rn and ^{4}He concentration in the Verde River were observed below visible spring input locations as well as three areas with no observed inputs (Fig. 11). These areas of increase in dissolved gases may represent areas of groundwater input to the stream beneath the streambed.

3.2.3. Stable isotopes

Stable isotopes can serve as indicators of recharge elevation, evaporation, and provide quantification of water from different sources. Stable isotope values in Verde River water collected in June 2016 become more depleted with input of groundwater along with an increase in ^{222}Rn and ^{4}He concentration (Fig. 12). The groundwater samples from springs in the study area had the lowest stable isotope values followed by Sycamore Creek (Fig. 13). The stable isotope value from the USGS Clarkdale gage from June 2016 plotted between the upstream most samples from this study in Mormon Pocket and the groundwater spring samples and had the lowest stable isotopic values of all surface water samples. The surface water samples from the Verde River plot

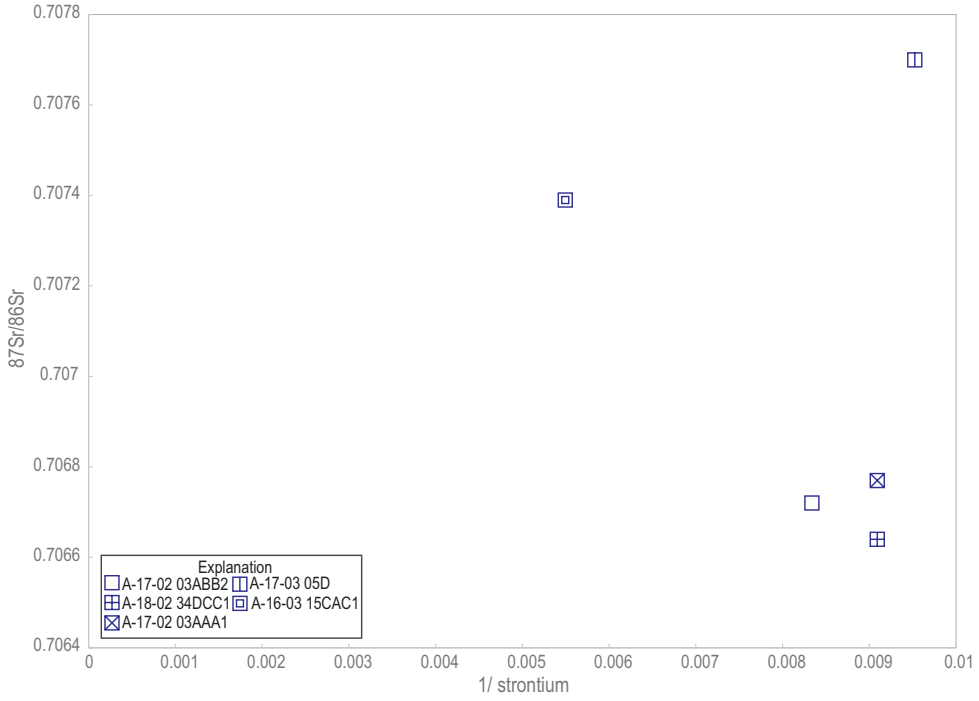

Fig. 8. Strontium concentration versus strontium isotope ratio for groundwater samples.

along the LMWL from Blasch et al., 2006 and may represent an evaporated signature. Two of the samples collected following the peak in discharge at the USGS Clarkdale gage (Figs. 10 and 13) were collected downstream of the crossing of a normal fault where there was a slight increase of ^{222}Rn concentration (Fig. 12). These two samples plot farther to the left compared with the other surface water samples and closer to the GMWL (Fig. 13).

Discharge increased 65 percent from the uppermost site in Mormon Pocket and the USGS Clarkdale gage between June 27 and 30, 2016. The proportion of groundwater at the USGS Clarkdale gage was computed using a simple 2 end-member mixing model as presented in Beisner et al. (2014) with a groundwater endmember of −11.75 and −82.2 for δ^{18}O and δ^{2}H respectively and a surface water endmember of the uppermost Verde River water with values of −9.85 and −73.5 for δ^{18}O and δ^{2}H respectively. The proportion of groundwater calculated for δ^{18}O was 57 percent and for δ^{2}H was 74 percent.

3.3. Modeling

Groundwater spring composition along the reach in June 2016 shows several isotopic indicators of regional groundwater flow with a high-elevation, low-evaporation, recharge zone including high noble gas recharge elevations, elevated radiogenic ^{4}He, and significantly lighter stable isotope signatures. The surface water composition in the

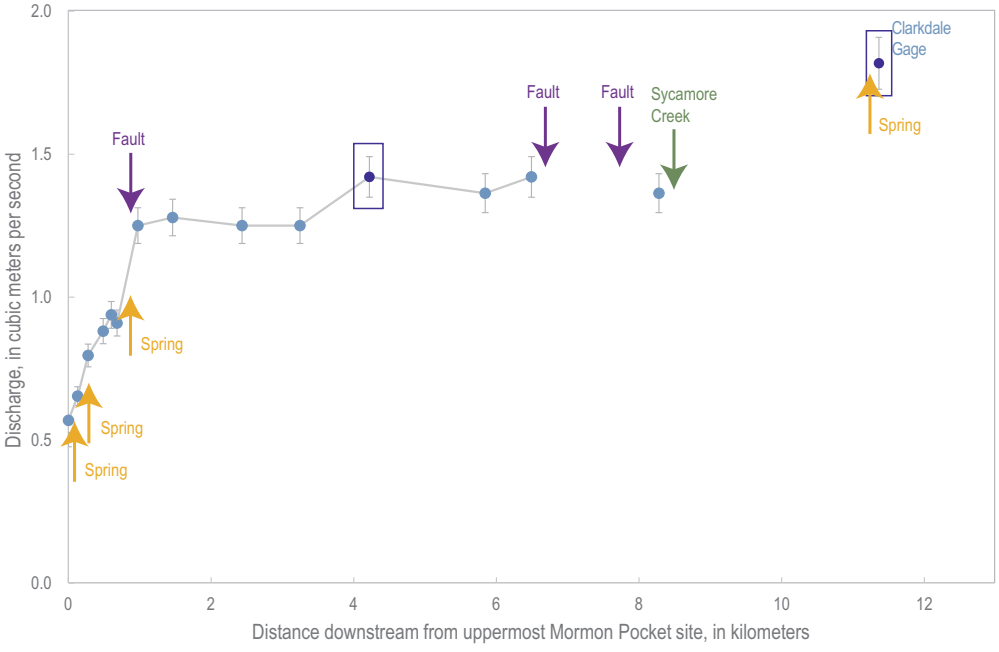

Fig. 9. Streamflow discharge change with distance downstream.

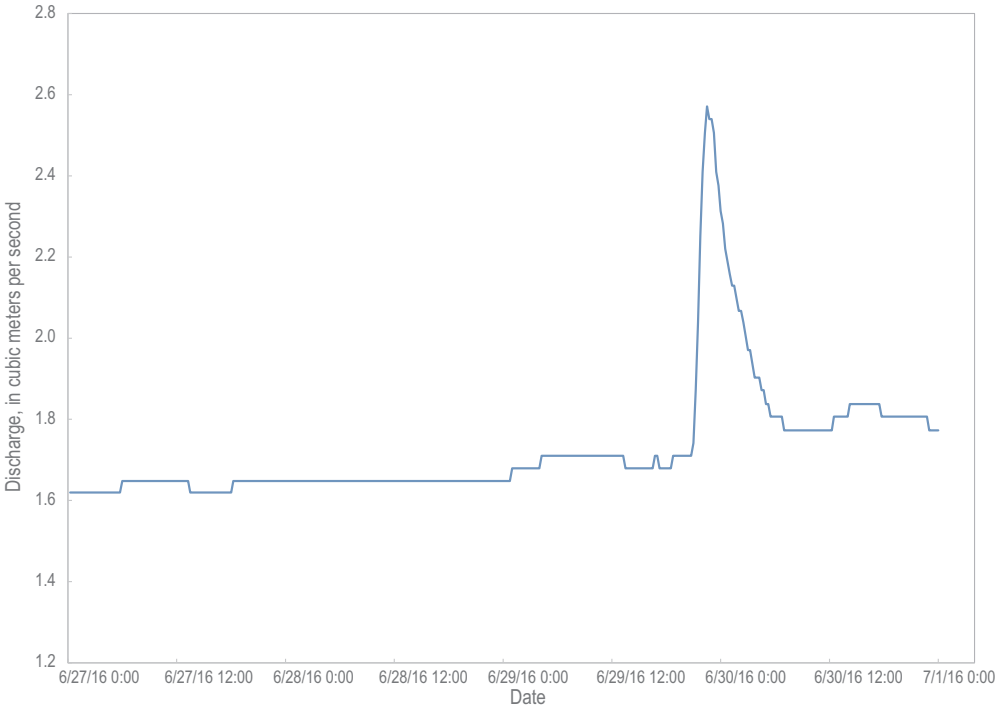

Fig. 10. Discharge from USGS Verde River near Clarkdale gage during June 2016 sampling.

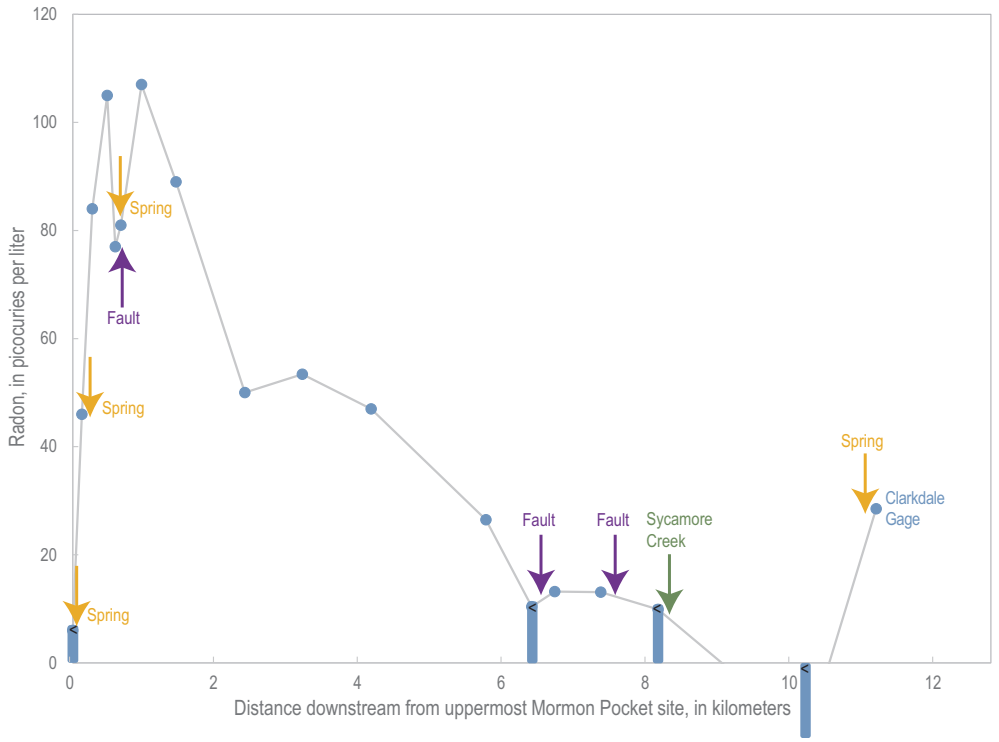

Fig. 11. Radon change with distance downstream from June 2016 sampling. Geology from DeWitt et al. (2008).

Verde River upstream of Mormon Pocket is more consistent with a higher evaporation, low elevation surface water and, in general, has higher conductivity, and is heavier isotopically.

The Verde systematically gained streamflow over the study reach during June 2016 (Fig. 14). The majority of this gain comes from subsurface discharge, as only one tributary joins the Verde along the reach. Estimated groundwater discharge along reach, determined by inversion against the stream discharge and ^{222}Rn concentrations shows most of the groundwater gain occurs in the first km of the reach (Figs. 14 and 15). Over this section we see a significant decrease in conductivity (Fig. 14) an increase in ^{222}Rn and ^{4}He (Fig. 15), and a shift to lighter isotopic compositions (Fig. 16). The trend in stream chemistry is indicative of addition of a regional groundwater source.

The model accurately captures the total discharge and ^{222}Rn, via inversion (Figs. 14 and 15). Because all water over 2 weeks in age should have relatively similar ^{222}Rn composition, this inversion

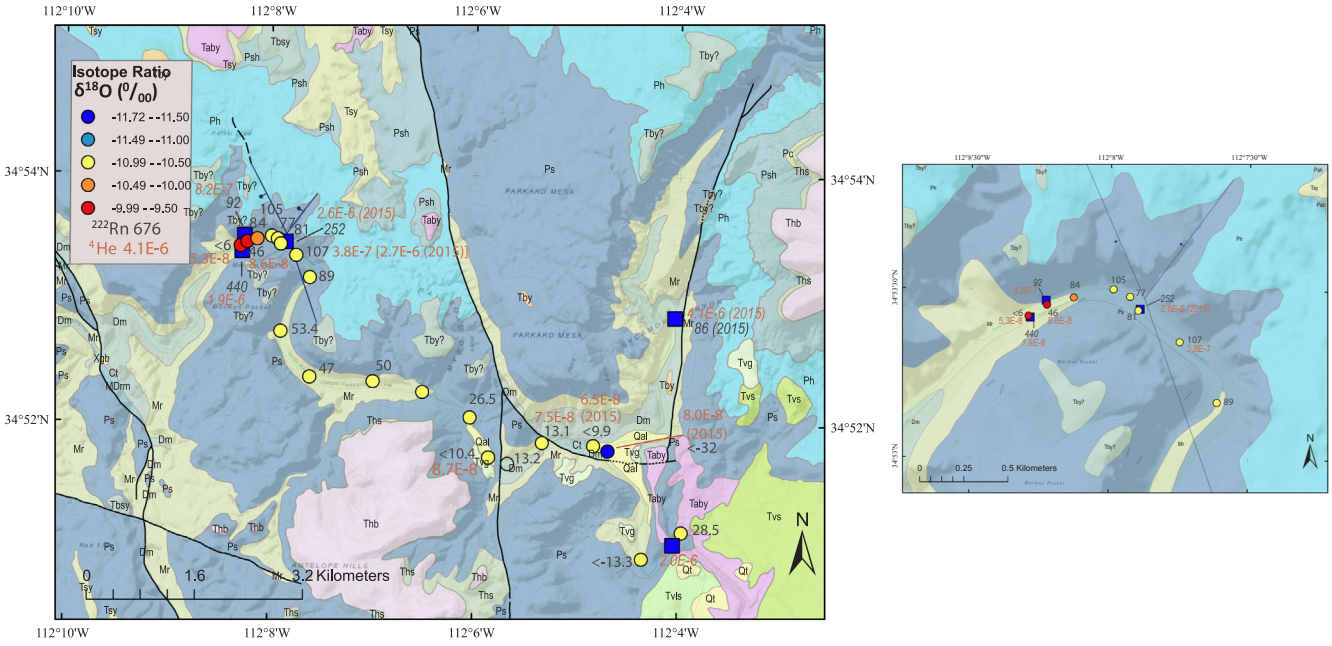

Fig. 12. Map of study area with isotope and gas data on geologic map with inset detail map of Mormon Pocket area. Geology from DeWitt et al. (2008) and blue fault lines from Lehner (1958). Circles represent surface water samples and squares and italic text represent springs. Description of geologic units on Fig. 1. (For interpretation of the references to colour in this figure legend, the reader is referred to the web version of this article.)

provides a reasonable and quantitative estimate of the total groundwater discharge to the stream over the reach, but does not distinguish between regional and other more shallow or local groundwater sources. Comparison of the subsequently estimated conductivity, stable isotope and ^{4}He composition of discharge groundwater with those observed in springs can be used to determine the dominant source of the groundwater discharge. The estimated groundwater discharge composition from the model was: specific conductance of 360 ± 40 µS/cm, ^{4}He of 1.1E−6 ± 4E−8 ccSTP/g, δ^{18}O of −11.4 ± 0.8 per mil, δ^2H of −81.5 ± 5 per mil; where the uncertainty in given by 95% linear confidence interval from the least-squares inversion.

Modeled conductivity, stable isotope signatures and ^{4}He fit the observed data from the Verde River well (Figs. 14–16). The three stable isotope samples collected in the Verde River following a small peak in surface water discharge on June 30 (Fig. 10) were on the order of 0.3 per mil for δ^{18}O and 3 per mil for δ^2H greater compared to river

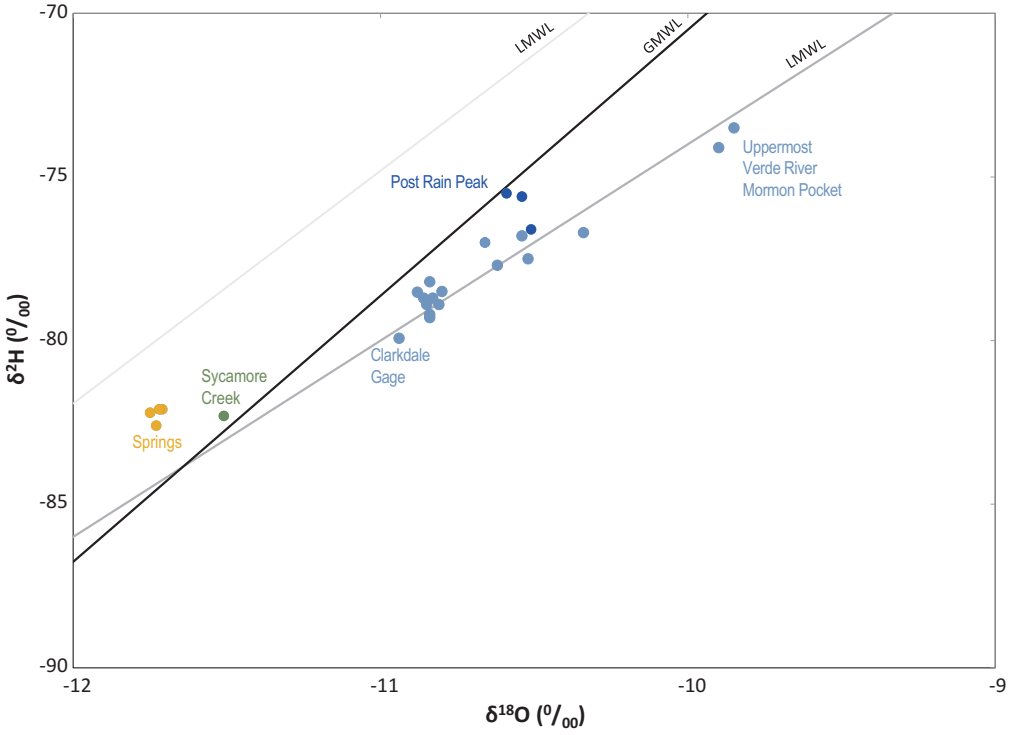

Fig. 13. Stable isotope graph with groundwater from spring and Verde River values. The global meteoric water line (GMWL) is from Craig, 1961, the light gray local meteoric water line (LMWL) is from Beisner et al. (2016), and the dark gray LMWL is from Blasch et al. (2006).

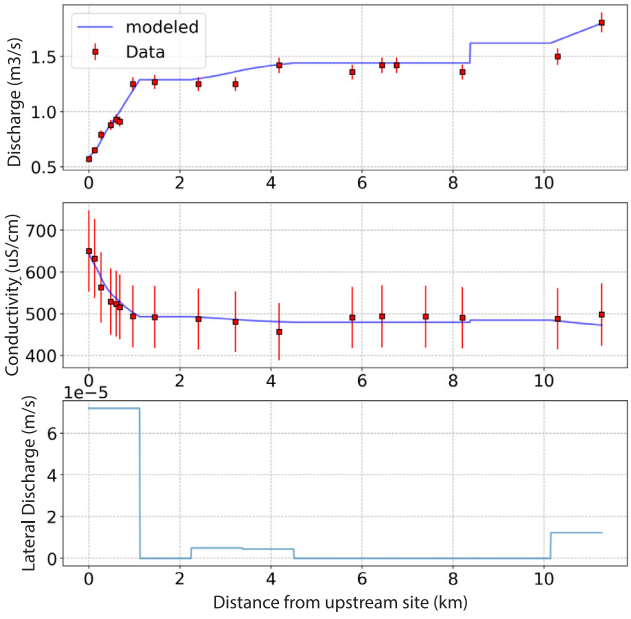

Fig. 14. Measured and modeled discharge (top), conductivity (middle), and best fit groundwater flux (bottom) along the study reach.

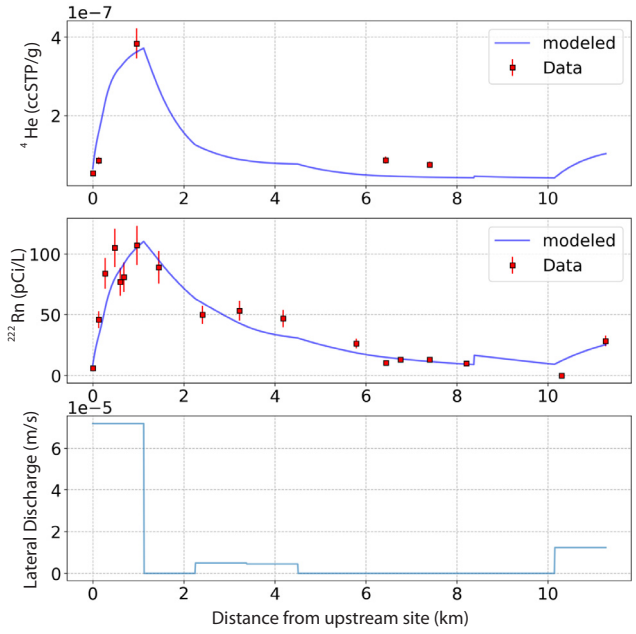

Fig. 15. Measured and modeled ^{4}He (top), ^{222}Rn (middle), and best fit groundwater flux (bottom) along the study reach.

samples prior to the peak and therefore are offset from the modeled data by a similar magnitude (Fig. 16).

The groundwater chemistry for springs discharging in Mormon Pocket during this study fall within the range of predicted groundwater composition from the model for specific conductance, $\delta^{18}O$, and $\delta^{2}H$, which provides a valuable check on the model. Modeled ^{4}He values are the same order of magnitude as several springs, and springs with an order of magnitude less ^{4}He may represent sites where degassing may be occurring prior to sample collection. The elevated ^{4}He concentration in groundwater, is two orders of magnitude above atmospheric compositions and thus indicative of significantly greater than 1000 years old. The isotopic compositions predicted by the model are significantly lighter than Verde River water, and agree well with spring water compositions, indicating a high elevation recharge area. Given the total

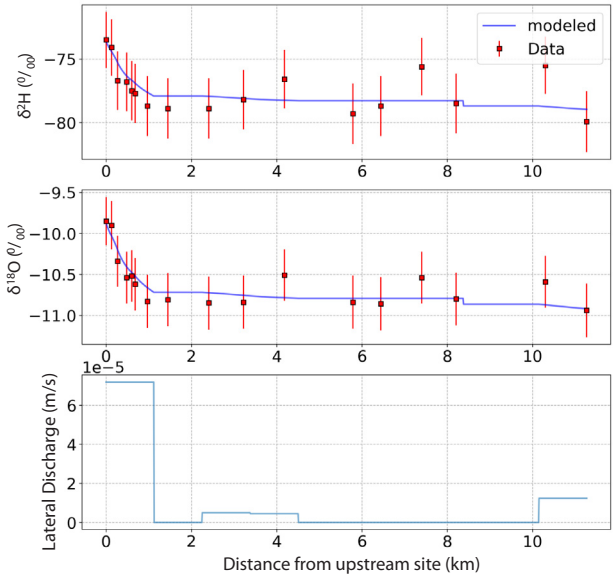

Fig. 16. Measured and modeled $\delta^{2}H$ (top), $\delta^{18}O$ (middle), and best fit groundwater flux (bottom) along the study reach.

isotopic composition of groundwater entering the stream, it is clear that all the groundwater discharge along the reach is from a regional source similar to that feeding the springs, and very little if any, groundwater discharge is from local sources such as local hyporheic exchange or alluvial groundwater discharge.

The parameter with the highest degree of uncertainty for the current study is the gas exchange coefficient. No tracer injection test was performed during the sampling period, significantly limiting our knowledge of this parameter. We estimated this parameter using published relationships derived large datasets of stream hydraulics and re-aeration coefficients. These relationships provide a reasonable estimate the for the gas exchange coefficient, but have significant uncertainty associated with them. We assess the uncertainty associated with the gas exchange coefficient using Bayesian analysis. Assuming our best groundwater inflows, we use a Markov Chain Monte Carlo (MCMC) sampling technique to sample from the posterior distribution of gas exchange coefficients which best fit the observed data. We assume a prior distribution, as a gamma distribution with the mean given by our calculated value (4.7 m/d) and a standard deviation of 1 m/d. We then use Gibbs sampler, which draws samples of the gas exchange coefficient, run the forward model and compare the modeled data to the observed data to estimate the likelihood of that gas exchange value.

We draw 1000 samples from posterior distribution, which gives us the best estimate of our knowledge of the gas exchange coefficient, given our observed data and the observation error. Our MCMC results indicate that the best fit mean gas exchange coefficient is 4.55 m/d, with a standard deviation of 0.4 m/d, and 95% linear confidence bounds of (3.85 m/d and 5.24 m/d). We estimate the predictive uncertainty due to uncertainty in the ^{222}Rn gas exchange coefficient, by re-running the groundwater inflow and then concentration estimation routines using the 95% confidence intervals. Using this analysis, the estimated groundwater concentrations for conductivity, ^{4}He and stable isotopes change by less than 1% – significantly less than the stated uncertainty in groundwater estimation least squares fit. These uncertainty results indicate that our estimate of groundwater isotopic composition is robust, and linear 95% confidence intervals derived from the least squares fit does an adequate job of characterizing the uncertainty of our estimate.

The age of streamflow is an open question in hydrology (McDonnell et al., 2010). Recent synthesis papers have demonstrated that streamflow and groundwater have short residence times globally (Gleeson

et al., 2016, Jasechko et al., 2016). However, continental scale surface and groundwater models indicate that the portion of old stream water is highly dependent upon the regional topographic, geologic and climatic conditions (Maxwell et al., 2016). More field studies, which directly investigate the role of regional groundwater discharge are required to understand the location, distribution and amount of regional groundwater discharge in streamflow generation. Here we use a unique set of isotopes, which allow for the identification of deep regional groundwater discharge. We modify the technique used by Gardner et al. (2011) and Smerdon et al. (2012) by directly estimating the groundwater inflow composition, rather than assuming it based upon nearby groundwater samples. This paradigm builds of that of Stolp et al. (2010) and Solomon et al. (2015), which both attempt to determine groundwater characteristics from stream samples. However, here we utilize a set of tracers which specifically target old water, rather than modern tracers. Our results give definitive evidence that the majority of streamflow addition to this reach of the Verde River comes from old, regional groundwater recharged at high elevations. Our results clearly illustrate that regional groundwater discharge can play an important role in streamflow generation. These field-based results are in agreement with theoretical papers that suggest arid watersheds, with high topography should be regional groundwater importers (Gleeson and Manning, 2008). Taking these lines of evidence together, we argue that more field-based investigations are required to fully constrain the role of regional groundwater discharge, especially in arid basins of high topographic relief.

4. Conclusions

We investigate a highly gaining reach of Verde River in Arizona to estimate the location of recharge and the role of regional groundwater discharge in streamflow generation in arid, mountainous landscapes. The Verde River more than doubles in discharge over the study reach. The majority of this increase is coming from groundwater discharge. Springs sampled in the area show lighter stable isotopic composition, lower conductivity, high noble gas recharge elevations and elevated radiogenic ^{4}He and ^{222}Rn when compared to local stream water. These isotopic signatures are consistent with a long residence time, regional flow path recharged at high elevations distal to the Verde River. Along the reach, the composition of the Verde River clearly shifts towards this regional end member. We used observed discharge and ^{222}Rn concentration along with stream transport modeling to estimate the spatial distribution of groundwater discharge to the Verde River, and estimate the conductivity, stable isotope and ^{4}He composition of the groundwater discharging to the stream. Groundwater discharge is focused in the upper kilometer of the reach. Modeled stable isotopic composition, conductivity and ^{4}He strongly indicate that long, regional groundwater flow paths are discharging to the stream, and that similar flow paths contribute to nearby springs. These modeling results show that virtually all of the streamflow gain over this section of the Verde River is coming from regional groundwater flow, with little to no indication of significant local hyporheic or alluvial groundwater discharge. Thus, streamflow generation over this reach can not be explained by local hillslope response or shallow, young groundwater additions. The tight spatial location of recharge, from a single regional source, indicates that streamflow generation in arid environments is highly heterogeneous and can be dominated by old water. These results indicate that more field-based study is required to constrain the role of regional groundwater in these systems, and that globally aggregated trends in stream and groundwater age may underestimate the role of old water in these settings. Once geochemistry has been established for groundwater in a study area, the model presented in this study can be useful for understanding contribution from groundwater to surface water resources.

Acknowledgements

The Verde Canyon Railroad graciously provided access to the remote sampling sites of the Verde River sampled in this study. This study was supported by Yavapai County, Cottonwood, Clarkdale, Sedona, Jerome, Camp Verde, and Yavapai Apache Nation matched by Arizona Department of Water Resources and the U.S. Geological Survey Cooperative Matching Funds.

Appendix A. Supplementary data

Supplementary data associated with this article can be found, in the online version, at https://doi.org/10.1016/j.jhydrol.2018.06.078.

References

Aeschbach-Hertig, W., Peeters, F., Beyerle, U., Kipfer, R., 1999. Interpretation of dissolved atmospheric noble gases in natural waters. Water Resour. Res. 35, 2779–2792.
Aeschbach-Hertig, W., Peeters, F., Beyerle, U., Kipfer, R., 2000. Palaeotemperature reconstruction from noble gases in ground water taking into account equilibration with entrapped air. Nature 405, 1040–1044.
ASTM D5072-09, 2016. In: Standard Test Method for Radon in Drinking Water. ASTM International, West Conshohocken, PA. http://dx.doi.org/10.1520/D5072-09R16. www.astm.org.
Ballentine, C.J., Hall, C.M., 1999. Determining paleotemperature and other variables by using an error-weighted, nonlinear inversion of noble gas concentrations in water. Geochim. Cosmochim. Acta 63, 2315–2336.
Ballentine, C.J., Burgess, R., Marty, B., 2002. Tracing fluid origin, transport and interaction in the crust. Rev. Mineral. Geochem. 47 (1), 539–614.
Bayer, R., Schlosser, P., Bonisch, G., Rupp, H., Zaucker, F., Zimmek, G., 1989. Performance and blank components of a mass spectrometric system routine measurement of helium isotopes and tritium by ^{3}He ingrowth method, Sitzungsberichte der Heidelberger Akademie der Wissenschaften. Heidelberg, Springer Verlag, Mathematisch-naturwissenschaftliche Klasse, pp. 241–279.
Beisner, K.R., Paretti, N.V., Brasher, A.M.D., Fuller, C.C., Miller, M.P., 2014. Assessment of metal and trace element contamination in water, sediment, plants, macroinvertebrates, and fish in Tavasci Marsh. In: US Geol. Surv. Sci. Invest. Report 2014–5069. Tuzigoot National Monument, Arizona, pp. 72. http://dx.doi.org/10.3133/sir20145069.
Beisner, K.R., Paretti, N.V., Tucci, R.S., 2016. Analysis of stable isotope ratios ($\delta^{18}O$ and $\delta^{2}H$) in precipitation of the Verde River watershed, Arizona, 2003 through 2014. In: US Geol. Surv. Open-File Report 2016–1053, http://dx.doi.org/10.3133/ofr20161053.
Bills, D.J., Flynn, M.E., Monroe, S.A., 2007. Hydrogeology of the Coconino Plateau and adjacent areas, Coconino and Yavapai Counties, Arizona. In: US Geol Surv Sci. Invest. Report 2005–5222.
Blasch, K.W., Hoffmann, J.P., Graser, L.F., Bryson, J.R., Flint, A.L., 2006. Hydrogeology of the upper and middle Verde River watersheds, central Arizona. In: US Geol. Surv. Sci. Invest. Report 2005–5198, pp. 3.
Bullen, T.D., Krabbenhoft, D., Kendall, C., 1996. Kinetic and mineralogic controls on the evolution of groundwater chemistry and 87Sr/86Sr in a sandy silicate aquifer, northern Wisconsin. Geochim. Cosmochim. Acta 60 (10), 1807–1821.
Cey, B.D., 2009. On the accuracy of noble gas recharge temperatures as a paleoclimate proxy. J. Geophys. Res. 114, D04107. http://dx.doi.org/10.1029/2008JD010438.
Cook, P.G., Herczeg, A.L., 2000. In: Environmental Tracers in Subsurface Hydrology. Springer, US, pp. 529. http://dx.doi.org/10.1007/978-1-4615-4557-6.
Craig, H., 1961. Isotopic variations in meteoric waters. Science 133, 1702–1703.
DeWitt, E., Langenheim, V., Force, E., Vance, R.K., Lindberg, P.A., Driscoll, R.L., 2008. Geologic map of the Prescott National Forest and the headwaters of the Verde River, Yavapai and Coconino Counties, Arizona. US Geol. Surv. Sci. Invest. Map 2996 scale 1: 100,000, 100-p, pamphlet.
Domenico, P.A., Schwartz, F.A., 1990. In: Physical and Chemical Hydrogeology. Wiley, New York, pp. 824.
Frisbee, M.D., Phillips, F.M., Campbell, A.R., Liu, F., Sanchez, S.A., 2011. Streamflow generation in a large, alpine watershed in the southern Rocky Mountains of Colorado: is streamflow generation simply the aggregation of hillslope runoff responses? Water Resour. Res. 47 (6), W06512.
Frost, C.D., Toner, R.N., 2004. Strontium isotopic identification of water-rock interaction and ground water mixing. Groundwater 42 (3), 418–432.
Gardner, W.P., Susong, D.D., Solomon, D.K., Heasler, H.P., 2010. Snowmelt hydrograph interpretation: revealing watershed scale hydrologic characteristics of the Yellowstone Volcanic Plateau. J. Hydrol. 383 (3–4), 209–222.
Gardner, W.P., Harrington, G.a., Solomon, D.K., Cook, P.G., 2011. Using terrigenic 4He to identify and quantify regional groundwater discharge to streams. Water Resour. Res. 47 (6), 1–13.
Genereux, D.P., Nagy, L.A., Osburn, C.L., Oberbauer, S.F., 2013. A connection to deep groundwater alters ecosystem carbon fluxes and budgets: example from a Costa Rican rainforest. Geophys. Res. Lett. 40 (10), 2066–2070. http://dx.doi.org/10.1002/grl.50423.
Gilmore, T.E., Genereux, D.P., Solomon, D.K., Farrell, K.M., Mitasova, H., 2016. Quantifying an aquifer nitrate budget and future nitrate discharge using field data

from streambeds and well nests. Water Resour. Res. 52 (11), 9046–9065. http://dx.doi.org/10.1002/2016WR018976.
Gleeson, T., Befus, K., Jasechko, S., Luijendijk, E., Cardenas, M.B., 2015. Global volume and distribution of modern groundwater: groundwater age transport modeling results (data). https://doi.org/10.14288/1.0357987.
Gleeson, T., Befus, K.M., Jasechko, S., Luijendijk, E., Cardenas, M.B., 2016. The global volume and distribution of modern groundwater. Nat. Geosci. 9 (2), 161–164. http://dx.doi.org/10.1038/ngeo2590.
Gleeson, T., Manning, A.H., 2008. Regional groundwater flow in mountainous terrain: three-dimensional simulations of topographic and hydrogeologic controls. Water Resour. Res. 44 (10), W10403-.
Guyer, J.E., Wheeler, D., Warren, J.A., 2009. FiPy: partial differential equations with Python. Comput. Sci. Eng. 11 (3).
HabiMap Arizona, 2018, Arizona biotic communities, http://arizonaexperience.org/live-maps/habimap-arizona, accessed February 5, 2018.
Haitjema, H.M., Mitchell-Bruker, S., 2005. Are water tables a subdued replica of the topography? Groundwater 43 (6), 781–786. http://dx.doi.org/10.1111/j.1745-6584.2005.00090.x.
Harrington, G.a., Payton, Gardner W., Munday, T.J., 2013. Tracking groundwater discharge to a large river using tracers and geophysics. Groundwater 52 (6), 837–852. http://dx.doi.org/10.1111/gwat.12124.
Hrachowitz, M., Benettin, P., van Breukelen, B.M., Fovet, O., Howden, N.J.K., Ruiz, L., van der Velde, Y., Wade, A.J., 2016. Transit times-the link between hydrology and water quality at the catchment scale. WIREs Water 3, 629–657. http://dx.doi.org/10.1002/wat2.1155.
Hunt, A.G., 2015. Noble Gas Laboratory's standard operating procedures for the measurement of dissolved gas in water samples. book 5, chap. A11 In: US Geol. Surv. Tech. and Methods, http://dx.doi.org/10.3133/tm5A11.
Jasechko, S., Kirchner, J.W., Welker, J.M., McDonnell, J.J., 2016. Substantial proportion of global streamflow less than three months old. Nat. Geosci. 9 (2), 126–129.
Johnson, R.H., DeWitt, E., Wirt, L., Manning, A.H., Hunt, A.G., 2012. Using geochemistry to identify the source of groundwater to Montezuma Well, a natural spring in Central Arizona, USA: part 2. Environ. Earth Sci. 67, 1837–1853. http://dx.doi.org/10.1007/s12665-012-1844-3.
Lee, J.Y., Hahn, J.S., 2006. Characterization of groundwater temperature obtained from the Korean national groundwater monitoring stations: implications for heat pumps. J. Hydrol. 329, 514–526.
Lehner, R.E., 1958. Geology of the Clarkdale quadrangle, Arizona. US Geol. Surv. Bull. 1021–N, 511–592.
Manga, M., 1996. Hydrology of spring dominated streams in the Oregon Cascades. Water Resour. Res. 32 (8), 2432–2439.
Manning, A.H., Solomon, D.K., 2003. Using noble gases to investigate mountain-front recharge. J. Hydrol. 275, 194–207.
Maxwell, R.M., Condon, L.E., Kollet, S.J., Maher, K., Haggerty, R., Forrester, M.M., 2016. The imprint of climate and geology on the residence times of groundwater. Geophys. Res. Lett. http://dx.doi.org/10.1002/2015GL066916.
McDonnell, J.J., McGuire, K., Aggarwal, P., Beven, K.J., Biondi, D., Destouni, G., Dunn, S., James, A., Kirchner, J., Kraft, P., Lyon, S., Maloszewski, P., Newman, B., Pfister, L., Rinaldo, A., Rodhe, A., Sayama, T., Seibert, J., Solomon, K., Soulsby, C., Stewart, M., Tetzlaff, D., Tobin, C., Troch, P., Weiler, M., Western, A., Wörman, A., Wrede, S., 2010. How old is streamwater? Open questions in catchment transit time conceptualization, modelling and analysis. Hydrol. Process. 24 (12), 1745–1754. http://dx.doi.org/10.1002/hyp.7796.
McDonnell, J.J., Beven, K., 2014. Debates-The future of hydrological sciences: a (common) path forward? A call to action aimed at understanding velocities, clerities and residence time distributions of the headwater hydrograph. Water Resour. Res. 50, 5342–5350. http://dx.doi.org/10.1002/2013WR015141.
Raymond, P.A., Zappa, C.J., Butman, D., Bott, T.L., Potter, J., Mulholland, P., Laursen, A.E., McDowell, W.H., Newbold, D., 2012. Scaling the gas transfer velocity and hydraulic geometry in streams and small rivers. Limnol. Oceanogr.: Fluids Environ. 2, 41–53. http://dx.doi.org/10.1215/21573689-1597669.
Révész, K., Coplen, T.B., 2008a. Determination of the $\delta(^2H/^1H)$ of water: RSIL lab code 1574. In: Révész, K., Coplen, T.B. (Eds.), Methods of the Reston stable isotope laboratory. US Geol. Surv. Tech. and Methods, book 10, chap C1. USGS, Reston, VA, pp. 27.
Révész, K., Coplen, T.B., 2008b. Determination of the $\delta(^{18}O/^{16}O)$ of water: RSIL lab code 489. In: Révész, K., Coplen, T.B. (Eds.), Methods of the Reston stable isotope laboratory. US Geol. Surv. Tech. and Methods. USGS, Reston, VA book 10, chap C2.
Smerdon, B.D., Gardner, W. Payton, Harrington, G.a., Tickell, S.J., 2012. Identifying the contribution of regional groundwater to the baseflow of a tropical river (Daly River, Australia). J. Hydrol. 464–465, 107–115.
Solder, J.E., Stolp, B.J., Heilweil, V.M., Susong, D.D., 2016. Characterization of mean transit time at large springs in the Upper Colorado River Basin, USA: a tool for assessing groundwater discharge vulnerability. Hydrogeo. J. 24 (8), 2017–2033. http://dx.doi.org/10.1007/s10040-016-1440-9.
Solomon, D.K., Gilmore, T.E., Solder, J.E., Kimball, B., Genereux, D.P., 2015. Evaluating an unconfined aquifer by analysis of age-dating tracers in stream water. Water Resour. Res. 51 (11), 8883–8899. http://dx.doi.org/10.1002/2015WR017602.
Stolp, B.J., Solomon, D.K., Suckow, A., Vitvar, T., Rank, D., Aggarwal, P.K., Han, L.F., 2010. Age dating base flow at springs and gaining streams using helium-3 and tritium: Fischa-Dagnitz system, southern Vienna Basin, Austria. Water Resour. Res. 46 (7).
Tague, C., Grant, G.E., 2009. Groundwater dynamics mediate low-flow response to global warming in snow-dominated alpine regions. Water Resour. Res. 45 (W07421). http://dx.doi.org/10.1029/2008WR007179.
Turnipseed, D.P., Sauer, V.B., 2010. In: Discharge measurements at gaging stations: US Geol. Surv. Tech. and Methods book 3, chap. A8, pp. 87.
Ulrich, G.E., Billingsley, G.H., Hereford, R., Wolfe, E.W., 1984. Map showing geology, structure, and uranium deposits of the Flagstaff 1° x 2° quadrangle, Arizona. In: US Geol Surv Misc Invest Series Map I-1446.
U.S. Geological Survey, variously dated. In: National field manual for the collection of water-quality data: US Geol. Surv. Tech. of Water-Resour. Invest., book 9, chaps. A1-A10. Available online at http://pubs.water.usgs.gov/twri9A.
Verde River, Arizona. National Wild and Scenic Rivers System. https://www.rivers.gov/rivers/verde.php, Retrieved February 28, 2017.
"Verde River Greenway State Natural Area". Arizona State Parks. https://azstateparks.com/verde-river Retrieved February 28, 2017.
Weiss, R.F., 1968. Piggyback sampler for dissolved gas studies on sealed water samples. Deep-sea Res. 15, 695–699.
Zuber, A., Weise, S.M., Osenbruck, K., Grabczak, J., Ciezkowski, W., 1995. Age and recharge area of thermal waters in Ladek Spa (Sudeten, Poland) deduced from environmental isotope and noble gas data. J. Hydrol. 167, 327–349.